RSC Advances

ROYAL SOCIETY OF CHEMISTRY

www.rsc.org/advances

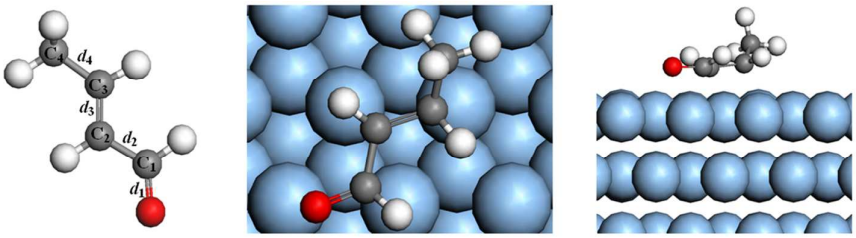

The parallel adsorption of crotonaldehyde molecule to the Pd(111) surface at the fcc-hcp site through the double bond of C=C and C=O is the most stable. The full hydrogenation mechanism follows the steps of $O \rightarrow C_2 \rightarrow C_3 \rightarrow C_1$ to generate the product of n-butane. And for the partial hydrogenation mechanism, the 1,4-addition is identified as a primary mechanism.

Adsorption and hydrogenation mechanism of crotonaldehyde on Pd(111) surface by periodic DFT calculations

Wei Shi, Lianyang Zhang, Zheming Ni*, Xuechun Xiao, Shengjie Xia

Laboratory of Advanced Catalytic Materials, College of Chemical Engineering and Materials Science, Zhejiang University of Technology, Hangzhou 310032, Zhejiang, China

* Corresponding author.

E–mail: jchx@zjut.edu.cn, nzm@zjut.edu.cn

Telephone number: 086–0571–88320373

Abstract:

The adsorption of crotonaldehyde molecule at Pd(111) surface and its mechanism of hydrogenation are elucidated by density-functional theory method (periodic DMol^3) at the GGA/PW91 level. All the pertinent species of different mechanisms were gathered to obtain their preferred adsorption sites. The activation energy and reaction energy of each step in different mechanisms were also calculated. Results show that the adsorption at the fcc-hcp site is the most stable state when the crotonaldehyde plane is in parallel to the Pd(111) surface through the double bond of C=C and C=O. The full hydrogenation mechanism follows the hydrogenation steps of $O \rightarrow C_2 \rightarrow C_3 \rightarrow C_1$ to generate the product of n-butane. For the partial hydrogenation mechanism, the 1,4-addition is identified as a primary mechanism to yield butenal, which further tautomerizes to n-butanal readily. Moreover, no matter what kind of dominant mechanism it is, the first hydrogenation process is the rate-determining step and the reaction is exothermic, therefore reducing the temperature is beneficial to the hydrogenation reaction of crotonaldehyde.

Key words: Crotonaldehyde; Adsorption; Selective hydrogenation mechanism; Pd(111); Density functional theory

1. Introduction

Crotonaldehyde is a group of representative compound of α, β-unsaturated aldehydes[1-4] and it is also a ubiquitous environmental pollutant produced by cigarette smoking[5-8]. The selective hydrogenation process can offer an effective way to reduce

pollution and convert the crotonaldehyde into a series of important chemical intermediates[9-14], such as crotyl alcohol, butanal, butyl alcohol and so on. For this reason, most of the research which has been done in recent years focuses on the development of catalysts for selective hydrogenation of crotonaldehyde[15].

At present, precious metal catalyst is the common catalyst in the hydrogenation of crotonaldehyde, which has superior catalytic activity and milder reaction conditions[16]. Among these precious metal catalysts, palladium (Pd) nanoparticles is one of the most effective precious metal catalysts which has the advantages of having high degree of dispersion and small average particle size[17,18]. It has been widely applied in the hydrogenation reactions of crotonaldehyde. Harraz *et al.*[17] synthesized the supported catalyst of Pd/PEG which presents a remarkable catalytic activity towards the selective hydrogenation of crotonaldehyde under mild conditions. Mclnroy *et al.*[19] investigated the hydrogenation process of crotonaldehyde which was catalyzed by a series of alumina-supported palladium catalysts. They found that the reaction followed the two steps are as follows: crotonaldehyde → butanal → butanol. Budroni *et al.*[20] researched the hydrogenation reaction of crotonaldehyde over Pd/Ni alloy catalysts, and the result suggested an effect on the hydrogenation reaction by ensembles of Pd atoms. Although there are extensive experimental researches on the hydrogenation reactions of crotonaldehyde, only a few reported its adsorption process and hydrogenation mechanism, due to the complexity of experiment and the limitation of characterization methods.

Density Functional Theory[21,22] can be widely used to calculate the adsorption

energy, structure parameter, activation energy and reaction energy in the process of different reactions. Ghosh *et al.*[23] carried out the thermodynamic research of DFT predicting the fragmentation behavior between crotonaldehyde and methacrolein. Also by DFT, Cao *et al.*[14] used three different methods to calculate the energy barrier of crotonaldehyde in the process of hydrogenation. They found that the turnover frequency of crotonaldehyde is close to the experiment value. In addition, they investigated the dominant hydrogenation mechanism of crotonaldehyde on Pt(111) surface, and proposed that the initial step of reactions begins with the oxygen atom.

In the present study, we used DFT method and Dmol3 program package to calculate the adsorption and hydrogenation mechanism of crotonaldehyde on clean Pd(111) surface. The properties of different adsorption sites are elucidated, which include structure parameter, adsorption energy. Furthermore, the likely reaction pathways of crotonaldehyde hydrogenation are also carried out to discover the primary mechanism. This work is devoted to provide a better understanding of the structural, energetic, catalytic and selective properties of Pd catalysts for the hydrogenation process of crotonaldehyde.

2. Computational Details

2.1. Calculation methods

All calculations were carried out in this study with the DMol3[24] program package by using the Materials Studio 5.5 of Accelrys Inc. The exchange and correlation energies were calculated by using the generalized gradient approximation

(GGA) of Perdew and Wang (PW91)[25-27]. The valence electron functions were expanded into a set of numerical atomic orbitals by a double-numerical basis with polarization functions (DNP). The convergence criterion of optimal geometry which were based on the energy, force and displacement convergence, were 1×10^{-5} Hartree, 2×10^{-3} Hartree and 5×10^{-4} nm, respectively. The transition state (TS) structures were computed using the Complete LST/QST tools[28] to investigate the minimum energy pathway for the hydrogenation of crotonaldehyde. In addition, each TS was verified by only one imaginary frequency. Throughout calculations, a Fermi smearing of 0.005 hartree was used to improve computational performance and all of the computations were performed with spin-polarization.

2.2. Surface model

In order to make a good balance among the calculation accuracy, calculation efficiency and the complexity of crotonaldehyde molecular, we modelled the Pd(111) surface by a periodic three-layer slab with a p(4×4) unit cell which contains 48 Pd atoms to study the adsorption and the hydrogenation of the crotonaldehyde molecular systems, as shown in Figure 1. Only one crotonaldehyde molecule was adsorbed on one side of the slab, in other words, the coverage is 1/16 mono-layer (ML). The vacuum region thickness between the repeat slabs was 1 nm, which was large enough to avoid interactions between different slabs. The layer and the vacuum region could form a unit which was repeated periodically in the space. During the simulating process, the top two layers and the middle layer of Pd(111) surface were allowed to

relax freely, and the bottom layer were kept fixed. Under the computational conditions above, the lattice parameters of Pd(111) surface was calculated to be 0.3893 nm, which is in good agreement with the experimental value of 0.3895 nm[29,30]. These results show that the method of calculation given in this paper is reliable.

(Insert Figure 1)

2.3. Molecule model

The crotonaldehyde molecule exists in the formation of the cis-trans isomerization[31]. As a result, the crotonaldehyde molecule has two isomers in total, as shown in Figure 2. We obtained the energies and structure parameters of different isomers in Table 1.

(Insert Figure 2)

(Insert Table 1)

From Table 1 we can see that no matter what kind of isomers they are, the calculation of bond length for free crotonaldehyde is in good agreement with the experimental value[31]. Meanwhile we found that the energy of s-trans-crotonaldehyde is higher than s-cis-crotonaldehyde and the bond length of s-trans-crotonaldehyde is

closer to the experimental value[31]. These phenomena suggests that the s-trans-crotonaldehyde is the optimized configuration and our computational method is proper to the system of crotonaldehyde molecule at the Pd(111) surface, which qualifies us for investigation of crotonaldehyde adsorption and hydrogenation mechanism on the Pd(111) surface.

3. Results and discussion

3.1. Adsorption energies and geometries analysis

The adsorption energy can be used to describe the variation of total energy of each species before and after adsorption. The signs and values of adsorption energy can indicate the possibility of adsorption. In the present work, the adsorption energy(E_{ads}) was calculated according to the equation:

$$E_{ads} = E_{(A/surface)} - (E_A + E_{surface})$$

where $E_{(A/surface)}$ is the total energy of the crotonaldehyde molecule adsorption system in the equilibrium state on Pd(111) surface; E_A and $E_{surface}$ are the total energies of the free crotonaldehyde molecule and clean Pd(111) surface, respectively. With this definition, a negative value corresponds to the stable adsorption on Pd(111) surface.

According to the structure of crotonaldehyde and the result that people had been studied[32]. There exist two categories of adsorption sites: (1) Independent adsorption of double bond: we consider the crotonaldehyde adsorbed on Pd(111) surface through the C=C bond or C=O bond in eight different adsorption sites, which include top, hcp,

fcc and bridge sites. (2) Cooperative adsorption of double bond: we consider the crotonaldehyde adsorbed on Pd(111) surface through the C=C bond and C=O bond in sixteen different adsorption sites. We have listed the adsorption energies of crotonaldehyde molecule on Pd(111) surface in Table 2.

(Insert Table 2)

From Table 2 we can see the adsorption structures that have been interconverted after the calculation and we found that the adsorption energies of crotonaldehyde were divided into three parts. The first and the second part are around -97 kJ/mol and -130 kJ/mol, which stand for the independent adsorption of C=C. The third part is around -156 kJ/mol, which represents the cooperative adsorption of C=C and C=O. Compared with the adsorption energies of three parts, we can find that the cooperative adsorption is superior to the independent adsorption. And the independent adsorption of C=O is the most unstable, it will change to the C=C adsorption or the cooperative adsorption of C=C and C=O. These results are in good agreement with the references[32]. The adsorption energy of initial site of bri-top is the lowest and its E_{ads} is -157.0 kJ/mol, which suggests that the initial site of bri-top, is the most stable adsorption configurations. Figure 3 displays the top view and side view of the most stable configurations of crotonaldehyde on Pd(111) surface.

(Insert Figure 3)

From Figure 3, it can be observed that the methyl tilted upward from the horizontal plane when the adsorption occurred. Moreover, the double bond of C=C and C=O have been transferred away from the initial adsorption site of bri-top. Finally, the crotonaldehyde molecule was adsorbed on fcc-hcp site through the double bond of C=C and C=O. Table 3 provides a list of calculated structural parameters of the most stable adsorption site of crotonaldehyde on Pd(111) surface. After adsorption, all the bond lengths of crotonaldehyde increased, which suggests that the energy of crotonaldehyde decreased and the adsorption of crotonaldehyde on Pd(111) surface could promote the hydrogenation reaction. Furthermore, the bond length of d_1 changes a lot, these phenomena imply that the reaction is most likely to occur on the double bond of C=O.

(Insert Table 3)

3.2. Hydrogenation mechanism of crotonaldehyde

(Insert Figure 4)

Based on the previous studies[33], we have already known that the crotyl alcohol was practically nil for the Pd catalyst when the reaction occurred. The hydrogenation of crotonaldehyde may proceed through a series of pathways and corresponding

intermediates, as depicted in Figure 4. The hydrogenation mechanism was classified into two types, which is consisted of partial hydrogenation and complete hydrogenation. For these two pathways, the partial hydrogenation produces butyraldehyde (FS9) or enol (FS8), while the complete hydrogenation produces butanol (FS14). We optimized the structures of reactants (IS) and products (FS) in Figure 4, and then searched TS between them. The activation energies and reaction energies at TS are tabulated in Table 4. Among different reaction mechanisms, the initial step is always the coadsorption of crotonaldehyde and hydrogen, so we only compared the intermediate steps of hydrogenation process in Figure 4(Step1-Step3).

(Insert Table 4)

3.2.1. Full hydrogenation pathway

IS1*+H*→C_4H_7O* (FS1 or FS2 or FS3 or FS4)

The activation energies and reaction energies of IS, TS and FS in the mechanisms of step 1 are presented in Figure 5. It is clear to see that the hydrogen atom shifted away from fcc site and the crotonaldehyde molecule still adsorb on fcc-hcp site through the double bond of C=C and C=O when the hydrogenation reaction happens.

(Insert Figure 5)

For the product of FS1, the molecule of which rotated anticlockwise, and at the same time, the oxygen atom tilted upward. Finally, the FS1 adsorbed on fcc site through the double bond of C=C. The TS1 was also calculated between IS1 and FS1 in Figure 5. When the hydrogenation reaction occurred, the hydrogen atom shifted from the fcc site to the hollow site and the oxygen atom tilted upward slightly to form the bond of O-H. The activation energy and the reaction energy of FS1 were 73.2 kJ/mol and -34.2 kJ/mol, respectively.

For the product of FS2, the molecule of which rotated clockwise compared to the IS1. Meanwhile, the methylene that tilted upward and the bond of C-O was elongated downward after adsorption. As a result, the FS2 was adsorbed on top-bri site through the double bond of C=C and the oxygen atom. During the hydrogenation process, the hydrogen atom moved close to the C_1 gradually in order to form the methylene in TS2. The activation energy and the reaction energy of FS2 were 90.4 kJ/mol and 70.0 kJ/mol, respectively.

For the product of FS3, there was a huge distortion, which can be observed when the reaction happened. The most stable adsorption structure was the bridge site through the double bond of C=C in FS3. The hydrogen atom shifted to the bottom of C_2, while the functional group of methyl and methyne were folded up, as shown in TS3. The activation energy and the reaction energy of FS3 were 99.0 kJ/mol and 93.0 kJ/mol, respectively.

For the product of FS4, the distortion can be also observed, but the level of distortion was less than the FS3. The methyl moved upward, and then located on the

top of methylene. Finally, the FS4 adsorbed on bridge site through the double bond of C=O. The configurations of TS4 rotated anticlockwise to approach the hydrogen atom, and meanwhile the hydrogen atom shifted close to the bottom of C_3. These phenomena are helpful to form the bond of C_3-H. The activation energy and the reaction energy of FS4 were 109.1 kJ/mol and -23.7 kJ/mol, respectively.

As can be seen from Table 4 and Figure 5, the reaction energy of FS1 is the smallest as compared with FS2, FS3 and FS4, while the distortion of FS1 is less than other products, which indicates that the process of IS1 to FS1 is easier to occur in step 1, this result is in good agreement with the analysis of the structure parameters in crotonaldehyde. Moreover, in the view of thermodynamics, the relative energy of FS1 and FS4 are negative, so reducing the temperature is helpful for the reactions. On the contrary, the relative energy of FS2 and FS3 are positive, which suggests that the reaction is endothermic and higher temperature is favorable for the reactions.

FS1*+H*→C_4H_8O* (FS5 or FS8)

The product of FS1 is regarded as the optimal product in step 1. And further hydrogenation process would happen on the basis of FS1. The activation energies and reaction energies of IS, TS and FS in the mechanisms of step 2 are depicted in Figure 6. It can be seen that the initial step is the coadsorption of the FS1 and the hydrogen atom. After the adsorption, the hydrogen atom shifted away from fcc site and the hydroxy moved upwards, meanwhile the molecule of FS1 tilted along the horizontal to adsorbed on Pd(111) surface through the double bond of C=C.

(Insert Figure 6)

Compared with the differences between the IS2 and the FS5, we can see that the product of FS5 moved to the upper right and the molecule of which was parallel to the Pd(111) surface when the reaction happened. In addition, we calculated the configuration of TS5, as in Figure 6. The bond of C_2-H shifted upward and finally was perpendicular to surface plane. The dissociative hydrogen atom moved away from the surface to approach the C_2 in order to form another bond of C_2-H, while the distance between dissociative hydrogen atom and C_2 decreased from 0.2137 to 0.1641 nm. The activation energy and the reaction energy of FS5 were 21.2 kJ/mol and -60.5 kJ/mol, respectively.

For the product of FS8, the molecule of which rotated anticlockwise and the methyl shift upward. These phenomena result in the FS8 folded into the right angle, and ultimately the FS8 adsorbed on bridge site through the double bond of C=C. In TS8, the hydrogen atom and the methylene of C_3-H moved close to each other in order to form the methylene of H-C_3-H, and at the same time the methyl shifted upward gradually. The activation energy and the reaction energy of FS8 were 46.4 kJ/mol and -65.4 kJ/mol, respectively.

As a whole, the reaction energy of FS5 is 25.2 kJ/mol, which was smaller than FS8, meanwhile the steric hindrance of FS5 was less than FS8, which indicates that the reactivity of step 2 decreased with the increase of the steric hindrance, and the

process of IS2 to FS5 was easier to occur in the step 2. Moreover, the relative energy of FS5 and FS8 were negative, so that reducing the temperature was helpful for the reaction of step 2.

FS5*+H*→C_4H_9O* (FS10 or FS11)

The FS5, as the major product of step 2, would further react with hydrogen atom to generate the product of FS10 or FS11. The activation energies and reaction energies of IS, TS and FS in the mechanisms of step 3 were illustrated in Figure 7. It can be seen that the initial reaction channel for step 3 was the coadsorption of the FS5 and the hydrogen atom. When the reaction happened, the hydrogen atom shifted away from fcc site and the functional group of hydroxy, methylene and methyl in FS5 tilted upwards, while the methynes in FS5 tilted downwards. Finally, the molecule of FS5 adsorbed on Pd(111) surface through the atom of C_1 and C_3.

(Insert Figure 7)

For the product of FS10, the molecule of which tilted upwards on the basis of the hydroxy and the C atoms in FS10 almost stayed in alignment when seen from the side view. At last, the FS10 was adsorbed on hollow site through the functional group of hydroxy. In TS10, the dissociative hydrogen atom transferred from the fcc site to the neighboring hollow site and the relevant C_3–H distance was decreased to 0.1785 nm from 0.2428 nm in the IS3. The activation energy and the reaction energy of FS10

were 83.4 kJ/mol and -54.0 kJ/mol, respectively.

For the product of FS11, the configuration of methyl and methyne almost had no change. In contrast, the functional group of hydroxy and methylenes rotated along the bond of C_2-C_3. In TS11, the intermediate moved to the upper right and the dissociative hydrogen atom migrated to the adjacent hollow site to approach the C1, and finally a new C_1–H bond was formed. The activation energy and the reaction energy of FS11 were 100.5 kJ/mol and 15.0 kJ/mol, respectively.

By comparing the IS, TS and FS in Figure 7, we can see the activation energy of FS10 was 17.1 kJ/mol, which was smaller than FS11. The relative energy of FS10 was negative, which suggests that the reaction is exothermic and the lower temperature is helpful to the reaction. On the contrary, the relative energy of FS11 was positive, so that raising the temperature was favorable for the reactions. From kinetic and thermodynamic viewpoints, hydrogenation of FS5 on Pd(111) surface tends to yield FS10 rather than FS11 , that is FS10 is more competitive than FS11.

FS10*+H*→$C_4H_{10}O$* (FS14)

The FS10 is the optimal product in step3. We listed the activation energies and reaction energies of IS, TS and FS in the mechanisms of step 4 in Figure 8. The reaction of step 4 started with the FS10 locating on the Pd(111) surface through the oxygen atom of hydroxy and the hydrogen atom still staying on the fcc site.

(Insert Figure 8)

For the final product of FS14 in full hydrogenation pathway, the molecule of which slanted towards the Pd(111) surface through the oxygen atom, but meanwhile, the FS14 moved away from surface and the relevant Pd-O distance was elongated to 0.2164 nm from 0.1790 nm in the IS14. This phenomenon implies that the desorption of FS14 was in progress. In TS14, the intermediate almost had no change as compared with the IS4 and the dissociative hydrogen atom moved towards the adjacent hollow site in order to form the bond of C_1-H. This step had an activation energy of 93.1 kJ/mol and a reaction energy of 2.2 kJ/mol, respectively.

(Insert Figure 9)

The energetics that associated with the aforementioned optimal products in each steps are shown in the complete potential energy surface (PES) in Figure 9. We can see that the most favorable mechanism of full hydrogenation process was proposed as follows: the crotonaldehyde was hydrogenated to FS1 which then underwent a second hydrogenation to form FS5. The FS5 can further be hydrogenated to yield FS10, and finally the FS10 can undergo a fourth hydrogenation to generate the n-butane(FS14). Among in different steps in Figure 9, the whole reaction was exothermic and the generation of FS1 in step 1 was the rate-determining step.

3.2.2. Partial hydrogenation pathway

1,4 and 4,1-Addition

According to the readily tautomerization between the butenol and butanal, the 1,4 and 4,1-addition is regarded as a feasible mechanism in the hydrogenation process of crotonaldehyde. The 1,4-addition process and the formation of FS4 were discussed in detail in section of 3.2.1, so we only listed the activation energies and reaction energies of IS, TS and FS in the mechanism of 4,1-addition in Figure 10.

(Insert Figure 10)

The 4,1-addition reaction started evidently with the dissociative hydrogen atom located at the fcc site and the configuration of FS4 adsorbed at the bridge site through the double bond of C=O, ending with the FS8 resided at bridge site through the double bond of C=C. In TS41, the methyl tilted upwards and was located at the top of methylene, meanwhile, the dissociative hydrogen atom moved from the fcc site to the adjacent top site, tending to form a new H-O bond as reflected by the distance between the involved H and O atom(0.1667 nm). This step had an activation energy of 57.4 kJ/mol and a reaction energy of -75.9 kJ/mol, respectively.

(Insert Figure 11)

Based on the activation energies and the reaction energies, the detailed potential energy surface diagram of 1,4 and 4,1-addition on Pd(111) surface are plotted together

in Figure 11. The results indicate that no matter what kind of processes they are, the generation of the first step is always the rate-determining step and the reaction is exothermic, and therefore dropping the temperature is helpful to the 1,4 and 4,1-addition. Moreover, by comparing the energy barriers with different processes, the 1,4-addition is significantly easier to occur than the 4,1-addition does.

3,4 and 4,3-Addition

Compared with the 1,4 and 4,1-addition, the hydrogen atoms interacted with the double bond of C=C directly to yield n-butanal(FS9) in the process of 3,4 and 4,3-addition. The first hydrogenation of 3,4 and 4,3-addition were discussed in detail in section 3.2.1, so we only listed the activation energies and reaction energies of IS, TS and FS in the mechanism of second hydrogenation in Figure 12.

(Insert Figure 12)

In the 3,4-addition process, the reaction started with the coadsorption of the dissociative hydrogen atom and the FS3. The hydrogen atom moved from the fcc site to the adjacent bridge site and the configuration of FS3 adsorbed at the fcc site through the double bond of C=O, as can be seen in IS34. For the intermediate of TS34, the methyl transferred to the opposite direction as compared to the reactant in the IS34, meanwhile, the hydrogen atom shifted away from the bridge site in order to approach the C_3 atom, while the distance between the hydrogen atom and C_3 decreased from

0.4115 to 0.2775 nm. Finally, the FS9 was shaped like a trapezoid from the top view and adsorbed at the bridge site through the double bond of C=O. This process had an activation energy of 302.2 kJ/mol and a reaction energy of -137.8 kJ/mol, respectively.

For the process of 4,3-addition, the structure of the reactant and product are the same as the 4,1-addition and 3,4-addition, which was discussed above in detail. When the reaction occurred, the methyl moved downwards and the dissociative hydrogen atom shifted close to the C_2, and the relevant C_2-H distance is decreased to 0.1753 nm from 0.2490 nm in the TS43. The activation energy and the reaction energy of TS43 were 97.6 kJ/mol and -21.1 kJ/mol, respectively.

(Insert Figure 13)

In order to deeply understand the 3,4 and 4,3-addition process, the detailed potential energy surface diagram is presented in Figure 13. We found that the process of 4,3-addition requires lower energy barriers than the 3,4-addition does, and the 4,3-addition is evidently an endothermic step, which indicates that 4,3-addition is identified as a major mechanism in the process of 3,4 and 4,3-addition. The results can be explained by the lower steric hindrance of 4,3-addition, which increases their stabilization on the surface in the transition state. Furthermore, by comparing the mechanism of different partial hydrogenation process, we can found that the energy barriers of 1,4-addition are the lowest and the product of 1,4-addition is short-lived,

and then tautomerizes readily to the product of 3,4 and 4,3-addition. These phenomena implied that the mechanism of 1,4-addition is the primary mechanism during the partial hydrogenation process.

4. Conclusion

In this paper, we performed a systematical investigation of the adsorption process and hydrogenation mechanism of crotonaldehyde on the Pd(111) surface by density functional theory coupled with periodic slab models. The major findings can be summarized as follows.

Crotonaldehyde exists in two kinds of adsorption modes on Pd(111) surface and the cooperative adsorption is superior to the independent adsorption. The most stable adsorption structure is the parallel adsorption for the fcc-hcp site through the double bond of C=C and C=O. After crotonaldehyde is adsorbed, all the bond length of which increase and the H atom is mostly like to attack the C=O of crotonaldehyde when the hydrogenation reaction occurs.

For the full hydrogenation pathway, the dominant channel follows the hydrogenation steps of $O \rightarrow C_2 \rightarrow C_3 \rightarrow C_1$ to generate the product of n-butane. For the partial hydrogenation pathway, the 1,4-addition is identified as a primary mechanism to yield butenal, which further tautomerizes to n-butanal readily. And no matter what kind of dominant mechanisms it is, the reaction is exothermic, so that reducing the temperature is beneficial to the reactions. Moreover, the first hydrogenation process is the rate-determining step, whose energy barrier is the highest.

References

[1] J. F. Minambres, A. Marinas, J. M. Marinas and F. J. Urbano, *J. Catal*., 2012, **295**, 242-253.

[2] X. Hong, B. Li, Y. J. Wang, J. Q. Lu, G. S. Hu and M. F. Luo, *Appl. Surf. Sci*., 2013, **270**, 388-394.

[3] C. J. Kliewer, M. Bieri and G. A. Somorjai, *J. Am. Chem. Soc*., 2009, **131**, 9958-9966.

[4] H. Yoshitake and N. Saito, *Micropor. Mesopor. Mat*., 2013, **168**, 51-56.

[5] K. Frost-Pineda, B. K. Zedler, D. Oliveri, S. X. Feng, Q. W. Liang and H. J. Roethig, *Regul. Toxicol. Pharm*., 2008, **52**, 104-110.

[6] S. G. Carmella, M. L. Chen, A. Zarth and S. S. Hecht, *J. Chromatogr. B*., 2013, **935**, 36-40.

[7] B. C. Yang, Z. H. Yang, X. J. Pan, F. J. Xiao, X. Y. Liu, M. X. Zhu and J. P. Xie, *Toxicol. Lett*., 2013, **219**, 26-34.

[8] B. C. Yang, X. J. Pan, Z. H. Yang, F. J. Xiao, X. Y. Liu, M. X. Zhu and J. P. Xie, *J. Toxicol. Sci*., 2013, **38**, 225-235.

[9] K. J. A. Raj, M. G. Prakash, R. Mahalakshmy, T. Elangovan and B. Viswanathan, *J. Mol. Catal. A-Chem*., 2013, **366**, 92-98.

[10] H. Rojas, G. Diaz, J. J. Martinez, C. Castaneda, A. Gomez-Cortes and J. Arenas-Alatorre, *J. Mol. Catal. A-Chem*., 2012, **363**, 122-128.

[11] B. Li, X. Hong, J. J. Lin, G. S. Hu, Q. Yu, Y. J. Wang, M. F. Luo and J. Q. Qing, *Appl. Surf. Sci*., 2013, **280**, 179-185.

[12] A. Corma, M. E. Domine, L. Nemeth and S. Valencia, *J. Am. Chem. Soc.,* 2002, **124**, 3194-3195.

[13] A. Jayaprakash, V. Arjunan, S. P. Jose and S. Mohan, *Spectrochim. Acta. A*., 2011, **83**, 411-419.

[14] X. M. Cao, R. Burch, C. Hardacre and P. Hu, *Catal. Today*., 2011, **165**, 71-79.

[15] P. Concepcion, Y. Perez, J. C. Hernandez-Garrido, M. Fajardo, J. J. Calvino and A. Corma, *Phys. Chem. Chem. Phys*., 2013, **15**, 12048-12055.

[16] V. Gutierrez, F. Nador, G. Radivoy and M. A. Volpe, *Appl. Catal. A-Gen*., 2013, **464**, 109-115.

[17] F. A. Harraz, S. E. El-Hout, H. M. Killa and I. A. Ibrahim, *J. Mol. Catal. A-Chem*., 2013, **370**, 182-188.

[18] M. S. Lde, B. Hao, M. Neurock and R. J. Davis, *ACS. Catal*., 2012, **2**, 671-683.

[19] A. R. McInroy, A. Uhl, T. Lear, T. M. Klapoetke, S. Shaikhutdinov, S. Schauermann, G. Rupprechter, H. J. Freund and D. Lennon, *J. Chem. Phys*., 2011, **134**, 214704.

[20] G. Budroni, S. A. Kondrat, S. H. Taylor, D. J. Morgan, A. F. Carley, P. B. Williams and G. J. Hutchings, *Catal. Sci. Technol*., 2013, **3**, 2746-2754.

[21] D. W. Heermann, *Computer Simulation Methods in Theoretical Physics*, Springer-Verlag, 1990.

[22] A. R. Leach, *Molecular Modelling: Principles and Applications*, Addison Wesley Longman Limitted Press, 2001.

[23] A. K. Ghosh, A. Chattopadhyay, A. Mukhopadhyay and T. Chakraborty, *Chem.*

Phys. Lett., 2013, **561**, 24-30.

[24] B. Delley, *J. Chem. Phys*., 2000, **113**, 7756-7764.

[25] J. P. Perdew, J. A. Chevary, S. H. Vosko, K. A. Jackson, M. R. Pederson, D. J. Singh and C. Fiolhais, *Phys. Rev. B*., 1992, **46**, 6671-6687.

[26] J. A. White, D. M. Bird, M. C. Payne and I. Stich, *Phys. Rev. Lett*., 1994, **73**, 1404-1407.

[27] J. P. Perdew and Y. Wang, *Phys. Rev. B*., 1992, **45**, 13244-13249.

[28] T. A. Halgren and W. N. Lipscomb, *Chem. Phys. Lett*., 1977, **49**, 225.

[29] C. Kittel C, *Solid State Physics*, John Wiley & Sons, 1976.

[30] S. W. Mai, G. D. Zhou and W. J. Li, *Advanced inorganic structural chemistry*, Peking University Press, 2001.

[31] J. Haubrich, D. Loffreda, F. Delbecq, P. Sautet, A. Krupski, C. Becker and K. Wandelt, *J. Phys. Chem. C*., 2009, **113**, 13947–13967.

[32] F. Delbecq and P. Sautet, *J. Catal*., 1995, **152**, 217-236.

[33] B. C. Campo, M. A. Volpe, C. E. Gigola and E. Carlos, *Ind. Eng. Chem. Res*., 2009, **48**, 10234-10239.

Figure Captions

Fig. 1. The top(left) and side(right) view of Pd(111) surface models (4×4)

Fig. 2. The s-cis and s-trans structures of crotonaldehyde molecule

(a) represents s-cis-crotonaldehyde; (b) represents s-trans-crotonaldehyde

Fig. 3. The most stable configurations of crotonaldehydeon Pd(111) surface

(a) represents crotonaldehyde; (b) represents top view; (c)represents side view

Fig. 4. Different reaction pathways for the hydrogenation of crotonaldehyde

FS represents product

Fig. 5. The IS, TS, FS and relative energy (kJ/mol) of step 1 on Pd(111) surface

Note: FS1: Ea=73.2; ΔE=-34.2 FS2: Ea=90.4; ΔE=70.0

FS3: Ea=99.0; ΔE=93.0 FS4: Ea=109.1; ΔE=-23.7

Fig. 6. The IS, TS, FS and relative energy (kJ/mol) of step 2 on Pd(111) surface

Note: FS5: Ea=21.2; ΔE=-60.5 FS8: Ea=46.4; ΔE=-65.4

Fig. 7. The IS, TS, FS and relative energy (kJ/mol) of step 3 on Pd(111) surface

Note: FS10: Ea=83.4; ΔE=-54.0 FS11: Ea=100.5; ΔE=15.0

Fig. 8. The IS, TS, FS and relative energy (kJ/mol) of step 4 on Pd(111) surface

Note: FS14: Ea=93.1; ΔE=2.2

Fig. 9. Potential energy surface diagram of full hydrogenation mechanisms on Pd(111) surface

Fig. 10. The IS, TS, FS and relative energy (kJ/mol) of 4,1-addition on Pd(111) surface

Note: FS8 (4,1-addition): Ea=57.4; ΔE=-75.9

Fig. 11. Potential energy surface diagram of 1,4 and 4,1-addition on Pd(111) surface

Fig. 12. The IS, TS, FS and relative energy (kJ/mol) of 3,4 and 4,3-addition on Pd(111) surface

Note: FS9 (3,4-addition): Ea=302.2; ΔE=-137.8

FS9 (4,3-addition): Ea=97.6; ΔE=-21.1

Fig. 13. Potential energy surface diagram of 3,4 and 4,3-addition on Pd(111) surface

Table Captions

Table 1 Structure parameters of cis-transcrotonaldehyde molecule

Table 2 Adsorption energy(E_{ads}) ofcrotonaldehyde molecule on Pd(111) surface

Table 3 Adsorption energy(E_{ads}) and structure parameters of the most stable adsorption site ofcrotonaldehydeon Pd(111) surface

Table 4 Activation energy (*Ea*) and reaction energy (ΔE) of elementary reactions on Pd(111) surface

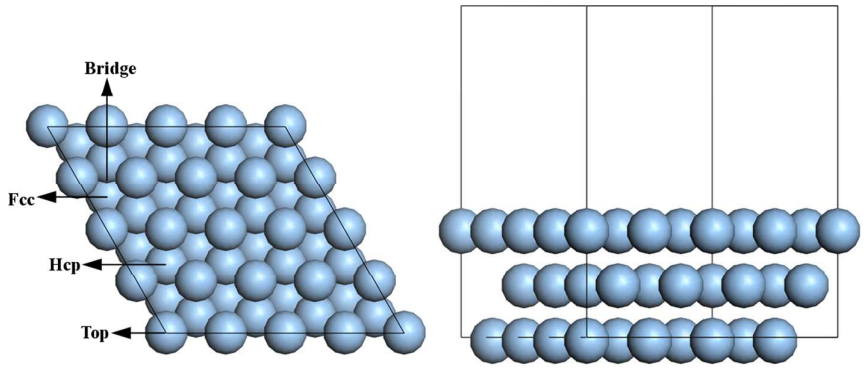

Fig. 1. The top(left) and side(right) view of Pd(111) surface models (4×4)

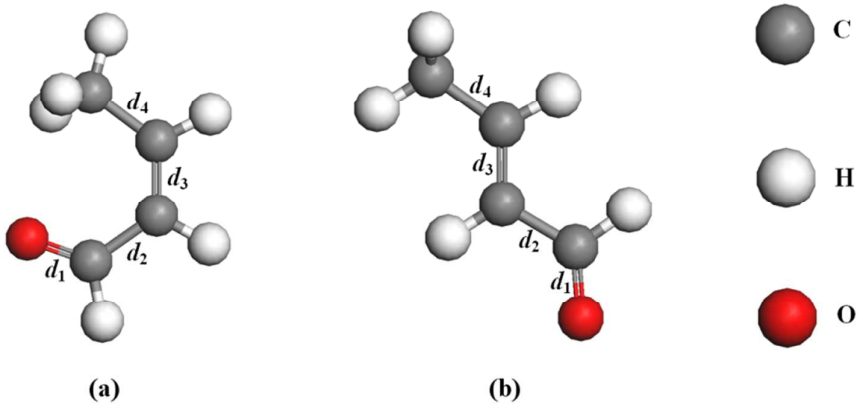

Fig. 2. The s-cis and s-trans structures of crotonaldehyde molecule

(a) representss-cis-crotonaldehyde; (b) represents s-trans-crotonaldehyde

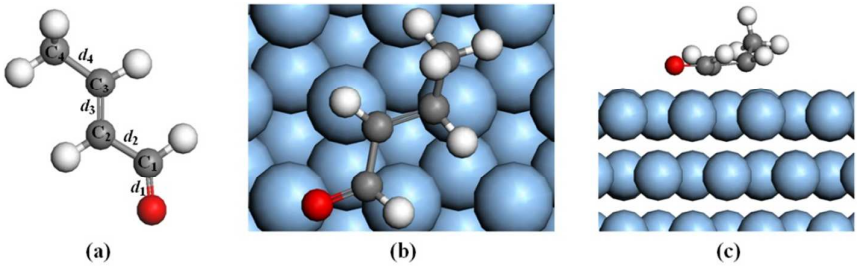

Fig. 3. The most stable configurations of crotonaldehydeon Pd(111) surface

(a) representscrotonaldehyde; (b) represents top view; (c)represents side view

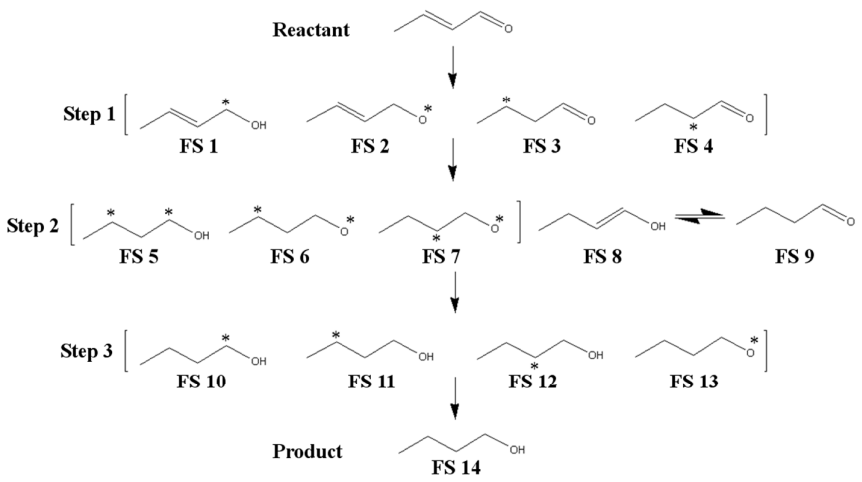

Fig. 4. Different reaction pathways for the hydrogenation of crotonaldehyde

Note: FS represents product

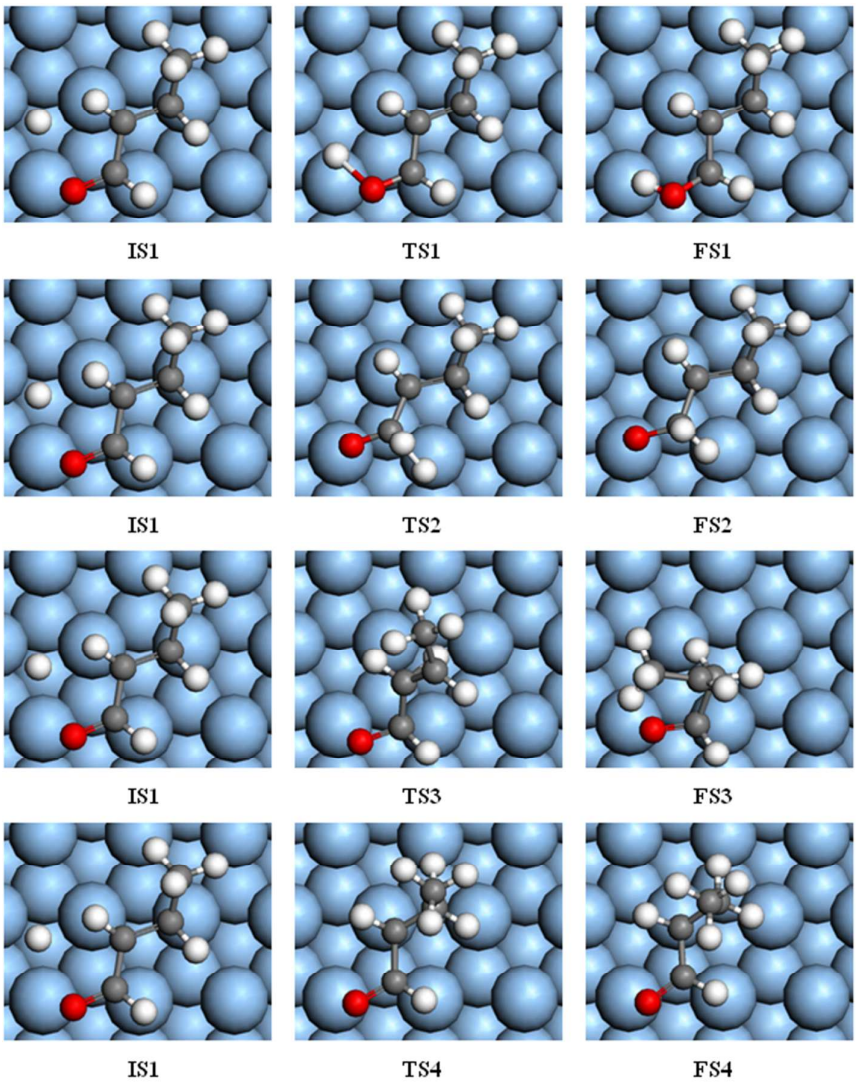

Fig. 5. The IS, TS, FS and relative energy (kJ/mol) of step 1 on Pd(111) surface

Note: FS1: *Ea*=73.2; *ΔE*=-34.2 FS2: *Ea*=90.4; *ΔE*=70.0

FS3: *Ea*=99.0; *ΔE*=93.0 FS4: *Ea*=109.1; *ΔE*=-23.7

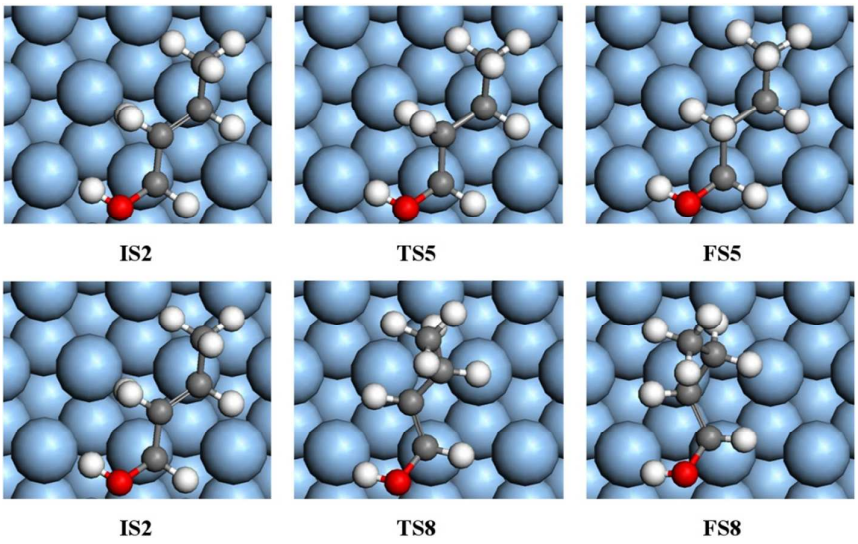

Fig. 6. The IS, TS, FS and relative energy (kJ/mol) of step 2 on Pd(111) surface

Note: FS5: *Ea*=21.2; *ΔE*=-60.5 FS8: *Ea*=46.4; *ΔE*=-65.4

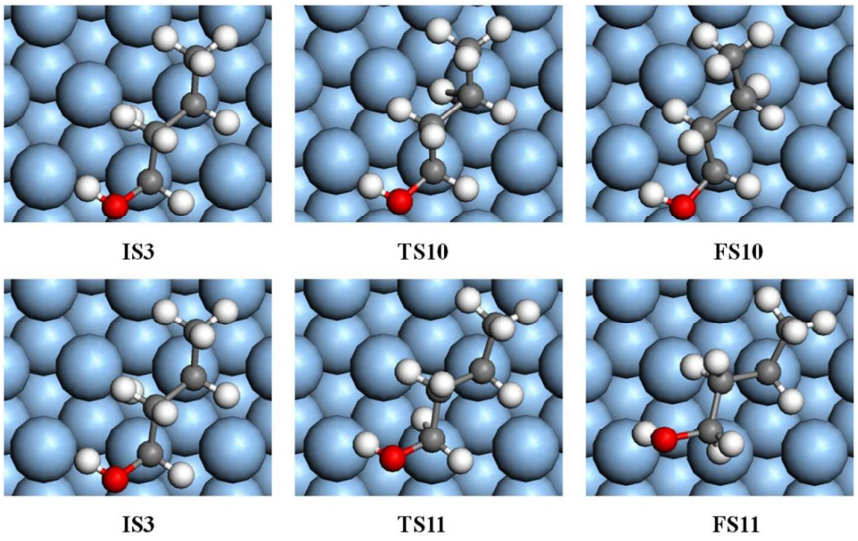

Fig. 7. The IS, TS, FS and relative energy (kJ/mol) of step 3 on Pd(111) surface

Note: FS10: *Ea*=83.4; *ΔE*=-54.0 FS11: *Ea*=100.5; *ΔE*=15.0

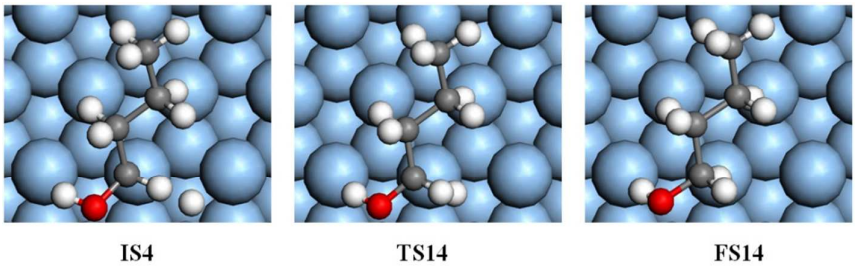

Fig. 8. The IS, TS, FS and relative energy (kJ/mol) of step 4 on Pd(111) surface

Note: FS14: *Ea*=93.1; *ΔE*=2.2

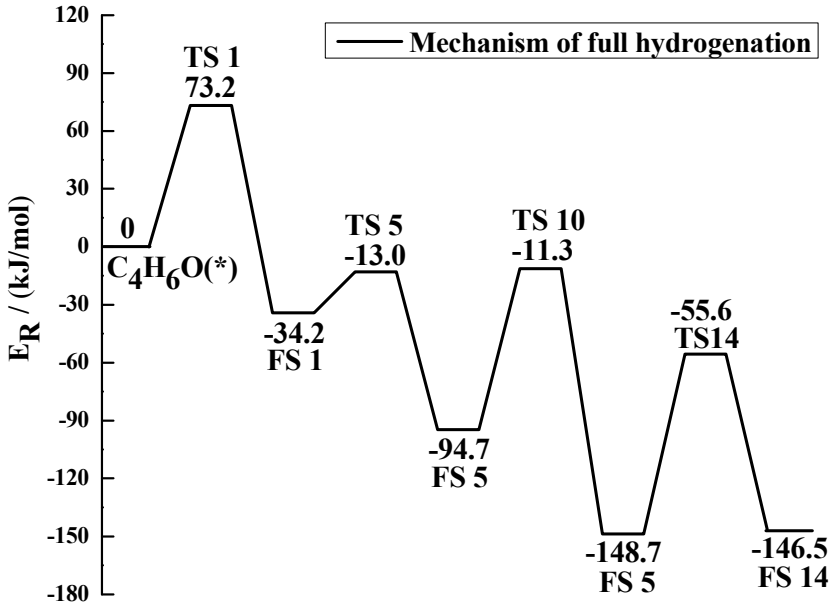

Fig. 9. Potential energy surface diagram of full hydrogenation mechanisms on Pd(111) surface

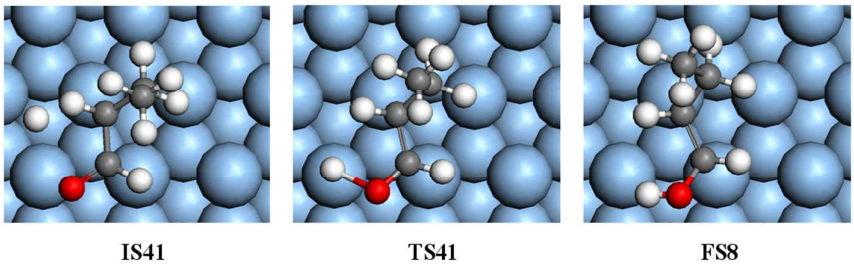

Fig. 10. The IS, TS, FS and relative energy (kJ/mol) of 4,1-addition on Pd(111)

surface

Note: FS8 (4,1-addition): *Ea*=57.4; *ΔE*=-75.9

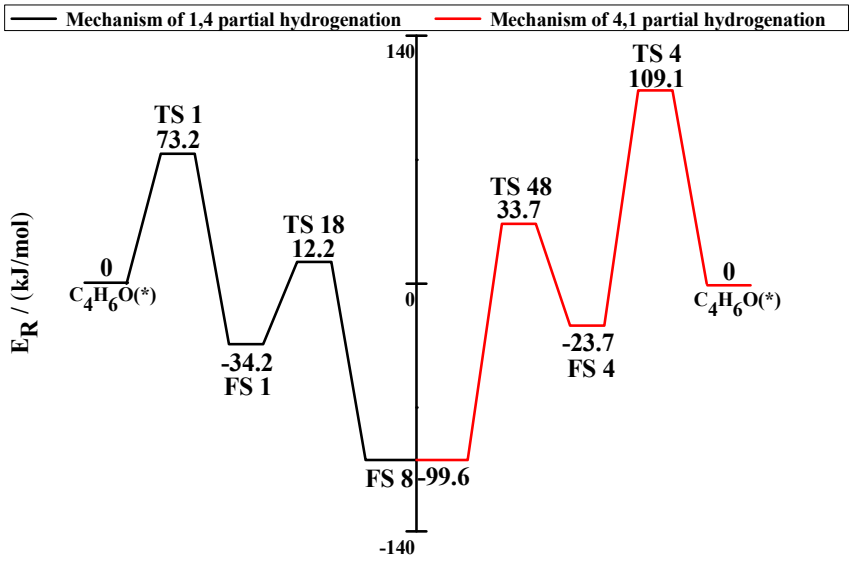

Fig. 11. Potential energy surface diagram of 1,4 and 4,1-addition on Pd(111) surface

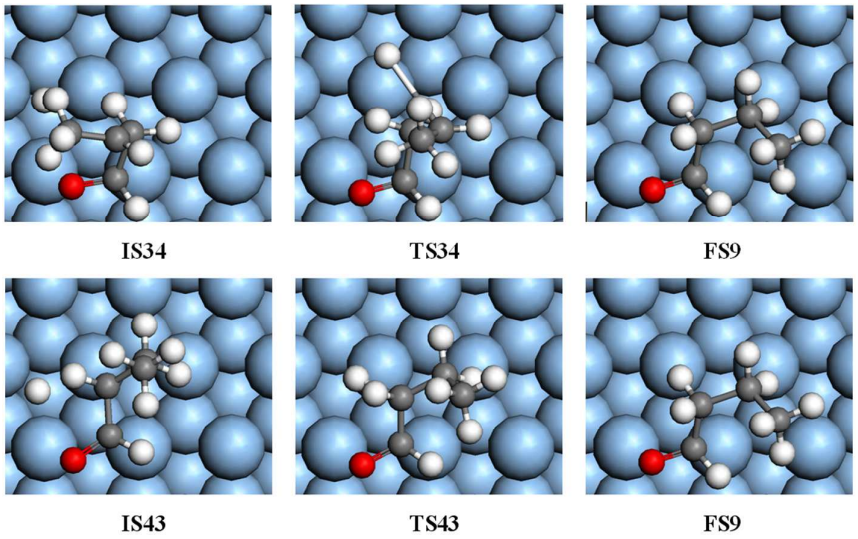

Fig. 12. The IS, TS, FS and relative energy (kJ/mol) of 3,4 and 4,3-addition on Pd(111)

surface

Note: FS9 (3,4-addition): *Ea*=302.2; *ΔE*=-137.8

FS9 (4,3-addition): *Ea*=97.6; *ΔE*=-21.1

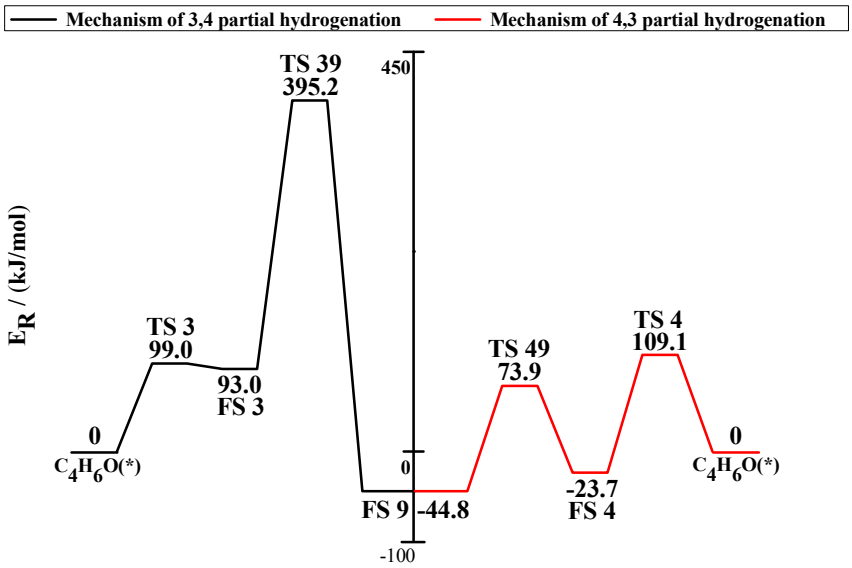

Fig. 13. Potential energy surface diagram of 3,4 and 4,3-addition on Pd(111) surface

Table 1 Structure parameters of cis-transcrotonaldehyde molecule

Model	E/(kJ/mol)	d_1	d_2	d_3	d_4
s-cis-crotonaldehyde	-607067.888	0.123	0.146	0.135	0.149
s-trans-crotonaldehyde	-607086.267	0.122	0.146	0.135	0.149
crotonaldehyde (experiment)	—	0.121	0.146	0.136	0.152

Table 2 Adsorption energy (E_{ads}) ofcrotonaldehyde molecule on Pd(111) surface

Independent adsorption	E_{ads}/(kJ/mol)	Cooperative	E_{ads}/(kJ/mol)
top(C=C)	-97.6	top(C=C)-top(C=O)	-154.2
hcp(C=C)	-155.4	top(C=C)-hcp(C=O)	-154.6
fcp(C=C)	-130.5	top(C=C)-fcc(C=O)	-98.3
bri(C=C)	-154.4	top(C=C)-bri(C=O)	-97.7
top(C=O)	-155.7	hcp(C=C)-top(C=O)	-134.0
hcp(C=O)	-130.8	hcp(C=C)-hcp(C=O)	-129.5
fcp(C=O)	-130.7	hcp(C=C)-fcc(C=O)	-155.4
bri(C=O)	-154.4	hcp(C=C)-bri(C=O)	-154.4
		fcc(C=C)-top(C=O)	-154.7
		fcc(C=C)-hcp(C=O)	-130.6
		fcc(C=C)-fcc(C=O)	-154.3
		fcc(C=C)-bri(C=O)	-130.3
		bri(C=C)-top(C=O)	-157.0
		bri(C=C)-hcp(C=O)	-133.2
		bri(C=C)-fcc(C=O)	-155.7
		bri(C=C)-bri(C=O)	-128.0

Note: The adsorption positions in table 2 represent the initial adsorption sites of crotonaldehyde

Table3 Adsorption energy(E_{ads}) and structure parameters of the most stable

adsorption site ofcrotonaldehydeon Pd(111) surface

Model	E_{ads}/(kJ/mol)	d_1	d_2	d_3	d_4
crotonaldehyde	—	0.122	0.146	0.135	0.149
crotonaldehyde /Pd(111)	-157.0	0.131	0.147	0.146	0.151
$\|\Delta d\|$	—	0.090	0.001	0.011	0.002

Table 4 Activation energy (*Ea*) and reaction energy (*ΔE*) of elementary reactions on Pd(111) surface

Reaction	*Ea*/(kJ/mol)	*ΔE*/(kJ/mol)
C_4H_6O*+H*→FS 1*+*	73.2	-34.2
C_4H_6O*+H*→FS 2*+*	90.4	70.0
C_4H_6O*+H*→FS 3*+*	99.0	93.0
C_4H_6O*+H*→FS 4*+*	109.1	-23.7
FS 1*+H*→FS 5*+*	21.2	-60.5
FS 1*+H*→FS 8*+*	46.4	-65.4
FS 5*+H*→FS 10*+*	83.4	-54.0
FS 5*+H*→FS 11*+*	100.5	15.0
FS 10*+H*→FS 14*	93.1	2.2
FS 4*+H*→FS 8*+*	57.4	-75.9
FS 3*+H*→FS 9*+*	302.2	-137.8
FS 4*+H*→FS 9*+*	97.6	-21.1